Electrochemistry Communications 71 (2016) 5–8

Contents lists available at ScienceDirect

Electrochemistry Communications

journal homepage: www.elsevier.com/locate/elecom

Poly(anthraquinonyl sulfide) cathode for potassium-ion batteries

Zelang Jian [a,1], Yanliang Liang [b,1], Ismael A. Rodríguez-Pérez [a], Yan Yao [b,c,*], Xiulei Ji [a,*]

[a] Department of Chemistry, Oregon State University, Corvallis, OR 97331-4003, United States
[b] Department of Electrical and Computer Engineering and Materials Science & Engineering Program, University of Houston, Houston, TX 77204, United States
[c] Texas Center for Superconductivity at the University of Houston, Houston, TX 77204, United States

ARTICLE INFO

Article history:
Received 30 June 2016
Received in revised form 21 July 2016
Accepted 21 July 2016
Available online 25 July 2016

Keywords:
Potassium-ion batteries
Organic material
Cathode
Polymer

ABSTRACT

Potassium-ion batteries (KIBs) are a promising sustainable energy storage technology due to the high abundance and low cost of potassium. Carbon anode materials for KIBs have seen great successes, but the development of cathode materials is yet to catch up. In this study, poly(anthraquinonyl sulfide) (PAQS) is evaluated as a cathode material for KIBs. It exhibits a high reversible capacity of 200 mAh/g, which is the highest value for a potassium storage cathode material. The cell shows two slopes averaged at 2.1 and 1.6 V vs. K^+/K. It shows a good cycling performance with the capacity retention of 75% after 50 cycles at a rate of C/10. These preliminary results indicate that PAQS is a promising cathode material for KIBs.

1. Introduction

Modular electrochemical energy storage is the absent enabler for large-scale installation of intermittent wind and solar energy sources. Li-ion batteries (LIBs) suffer the intrinsic drawback of lithium rarity and uneven distribution in the Earth's crust [1–3]. Despite their tremendous successes in portable electronics and electric vehicles, LIBs are not sustainable to be employed for purposes like load leveling, smart grid, and microgrids. It is inevitable to pursue alternative electrochemical devices based on elements that are Earth abundant. Recently, attention has been paid to potentially low-cost alkali metal-ion devices, including Na-ion batteries (NIBs) [1–3] and K-ion batteries (KIBs) [4,5]. Potassium-metal based devices, including K—O_2 batteries [6] and K—S batteries [7] also attracted attention, and aqueous-electrolyte-based KIBs employing Prussian blue cathode and anode were investigated as well [8,9]. Non-aqueous-electrolyte-based KIBs present unique advantages compared to LIBs and NIBs [5]. For the anode side of KIBs, our group and others have revealed that many bulk carbons, including graphite, soft carbon and hard carbon, demonstrate good capacity, e.g., ca. 270 mAh/g, high reversibility and good cyclability [5,10–12]. The K-carbon intercalation compounds represent the most stable type compared to other alkali-metal-carbon analogues. For example, the stage-one Na-graphite intercalation compounds (GICs) cannot even be formed due to the lack of favorable energetics between Na atoms and graphene sheets. For the electrolyte, K-ion diffusion in electrolytes is known to be faster than do Na-ion and Li-ion. The main challenge for KIBs may come from the cathode side due to the large strain caused by the bulky size of K-ions if crystalline minerals are used as cathodes.

Despite the difficulty, encouraging results have been obtained for cathodes in KIBs. To date, a few cathode materials were investigated [4,13,14]. Eftekhari demonstrated a Prussian blue cathode, which delivered a reversible capacity of ~78 mAh/g with excellent cycling [4]. Hu et al. and our group reported 3,4,9,10-perylene-tetracarboxylicacid–dianhydride (PTCDA) as a cathode, which showed a reversible capacity of 130 mAh/g in a voltage window of 3.5–1.5 V vs. K^+/K [13,14]. The journey to pursue suitable cathodes for KIBs has just started and more advanced cathode materials should be developed. Organic compounds had been wildly used as both a cathode and an anode for LIBs and NIBs due to their potentially low cost, renewability, and environmental friendliness [15–17]. Poly(anthraquinonyl sulfide) (PAQS) as a cathode for LIBs, NIBs and Mg-ion batteries presented a high capacity (~200 mAh/g) and good cycling stability [18–20]. It is intriguing to investigate the K-ion storage behavior in PAQS.

Herein, we synthesized PAQS by a very simple method and for the first time investigated its electrochemical K-ion storage properties for KIBs. The PAQS/K cells delivered a high reversible capacity of 200 mAh/g with a relatively stable cycling behavior.

2. Experimental

To the mixture of 1,5-dichloroanthraquinone (2.77 g, 10 mmol) and sodium sulfide nonahydrate (2.4 g, 10 mmol) was added methylpyrrolidone (25 mL) under argon. The stirred suspension was heated under argon at 200 °C overnight. After cooling down, the mixture was filtered and washed with hot water and acetone untill the filtrate became colorless. The "cake" was dried under vacuum at 120 °C

* Corresponding authors.
E-mail addresses: yyao4@uh.edu (Y. Yao), david.ji@oregonstate.edu (X. Ji).
[1] These authors equally contribute to the work.

http://dx.doi.org/10.1016/j.elecom.2016.07.011
1388-2481/

for 16 h to yield the product as brown powder (2.0 g, 86%). Powder X-ray diffraction (XRD) analysis was carried out on a Rigaku Ultima IV Diffractometer with Cu Kα irradiation (λ = 1.5406 Å). The Barrett-Joyner-Halenda (BJH) porous size distribution was calculated using the adsorption branch of N_2 sorption isotherms. Fourier transform infrared spectroscopy (FTIR) spectra were recorded on a Nicolet 6700 spectrometer (Thermo Electron). The morphology is examined by a FEI NOVA 230 high resolution scanning electron microscopy (SEM). The electrodes are composed of PAQS, Super P, and polyvinylidene fluoride (PVdF) with a mass ratio of 70:20:10. The slurry was cast onto Al foil and dried at 100 °C under vacuum for 10 h. Coin cells were assembled with potassium foil as the counter/reference electrode, a glass-fiber separator, and 0.5 M potassium bis(trifluoromethane sulfonyl) imide (KTFSI) in mixed dimethoxyethane and dioxolane solution (DOL: DME = 1:1 by volume) as an electrolyte in an argon-filled glovebox. The active mass loading was ~2 mg/cm^2. The electrochemical measurements were performed on a LAND system at room temperature. Cyclic voltammetry (CV) was conducted on a VMP-3 multi-channel workstation at a scanning rate of 0.1 mV/s.

3. Results and discussion

PAQS was synthesized by a Phillips method. The schematic diagram of PAQS is shown in Fig. 1a, which shows two carbonyl groups in one monomer. The PAQS structure was confirmed by XRD and FTIR spectrum. The crystalline peaks (Fig. 1b) appear at 12°, 22°, and 24°, which are consistent with previous literature. However, the peaks are much sharper than the reported ones, indicating a good crystalline structure [18]. SEM imaging shows a large particle size of >5 μm and the N_2 sorption results reveal the porous structure of PAQS, where the peak pore size from BJH calculation is ~38 nm and the Brunauer–Emmett–Teller (BET) surface area is 63 m^2/g (Fig. 1c). The FTIR spectrum is shown in Fig. 1d, where all the peaks are consistent with previous works [18]. The C═O and C═C stretching vibrations of the anthraquinonyl group locate at 1672 and 1568 cm^{-1}, respectively. The peaks at 1410 and 1127 cm^{-1} correspond to the stretching of the sulfur-disubstituted aromatic ring and the ring-sulfur, respectively. We do obtain anthraquinone-based PAQS by polycondensation.

First, we assembled PAQS/K cells with the electrolyte of 0.8 M KPF_6 in EC + DMC, which were cycled in the voltage range of 1.5–3.4 V vs. K^+/K (as shown in Fig. 2a). Although the cell shows high discharge (potassiation) capacity of 213 mAh/g, its reversible (depotassiation) capacity is only 137 mAh/g. The capacity fades seriously in the subsequent cycles. In contrast, the cell with 0.5 M KTFSI in DOL + DME electrolyte shows impressive initial discharge and charge capacity values of 211 and 190 mAh/g, respectively (Fig. 2b). It leads to a high coulombic efficiency of 90%. The subsequent charge/discharge curves almost overlap, especially for the charge curves, indicating good reversibility. Furthermore, the cell using the KTFSI/DOL + DME electrolyte shows much less polarization than the cell with KPF_6/EC + DMC electrolyte. Interestingly, the KTFSI/DOL + DME electrolyte shifts the potential of K^+ ion storage in PAQS to a slightly lower potential compared to the electrolyte of KPF_6/EC + DMC, particularly with a lack of capacity from 2.4 to 2.8 V vs. K^+/K. When the cell was cycled between 1.2 and 3.4 V vs. K^+/K in the KTFSI/DOL + DME electrolyte, it shows a high reversible capacity of 200 mAh/g with a first-cycle coulombic efficiency of 85% (Fig. 2c). The charge/discharge curves can be divided to two slopes, where each part is close to 100 mAh/g, corresponding to one K^+ ion insertion/extraction, and the average potential of the two slopes are 2.1 and 1.6 V vs. K^+/K. Note that PAQS/Na cells also show the two slopes, leading to a high capacity of 220 mAh/g [19]. However, PAQS/Li cells exhibit only one slope, which still presents a high capacity of 185 mAh/g [18]. All the PAQS/alkali metal cells present the insertion/extraction of about two alkali ions. The K^+ ion storage mechanism in PAQS is indicated in Fig. 2e, which is similar with PAQS/Na cells [19].

The CV curves (Fig. 2d) also show the two couples of redox peaks, where the initial cathodic peaks are at 1.68 and 1.38 V vs. K^+/K and the subsequent cathodic peaks shift to 1.87 and 1.45 V vs. K^+/K, which are slightly lower than the average galvanostatic discharge potentials for the two slopes, respectively. All the anodic curves in different cycles

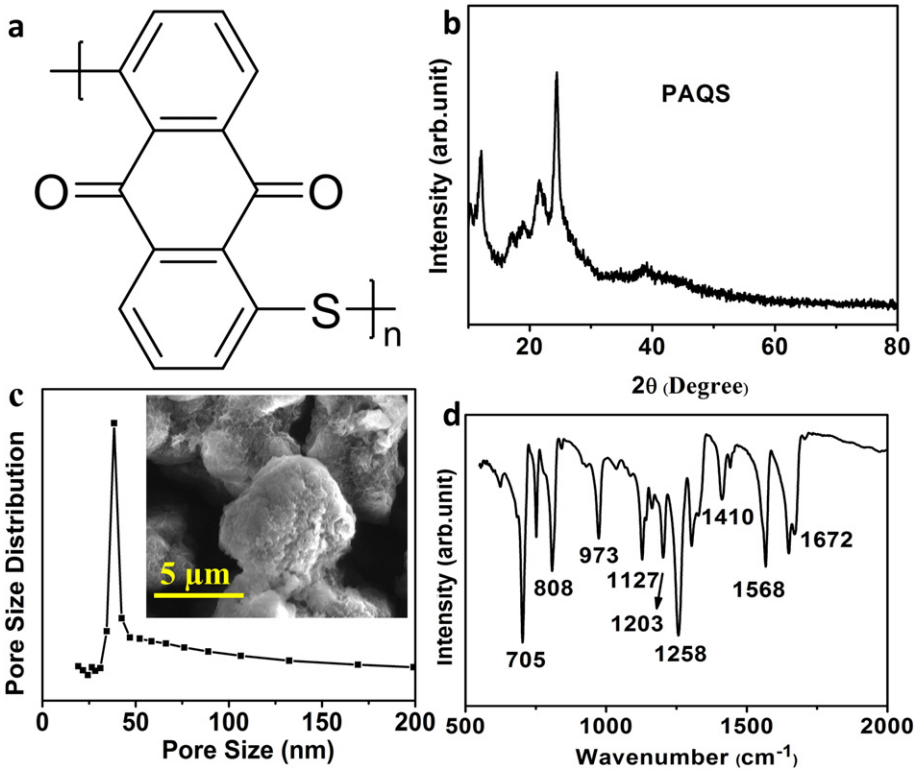

Fig. 1. Characterizations of PAQS. (a) Unit molecular structure of PAQS, (b) Wide angle XRD pattern, (c) Pore size distribution (inset is the SEM image) and (d) FTIR spectrum.

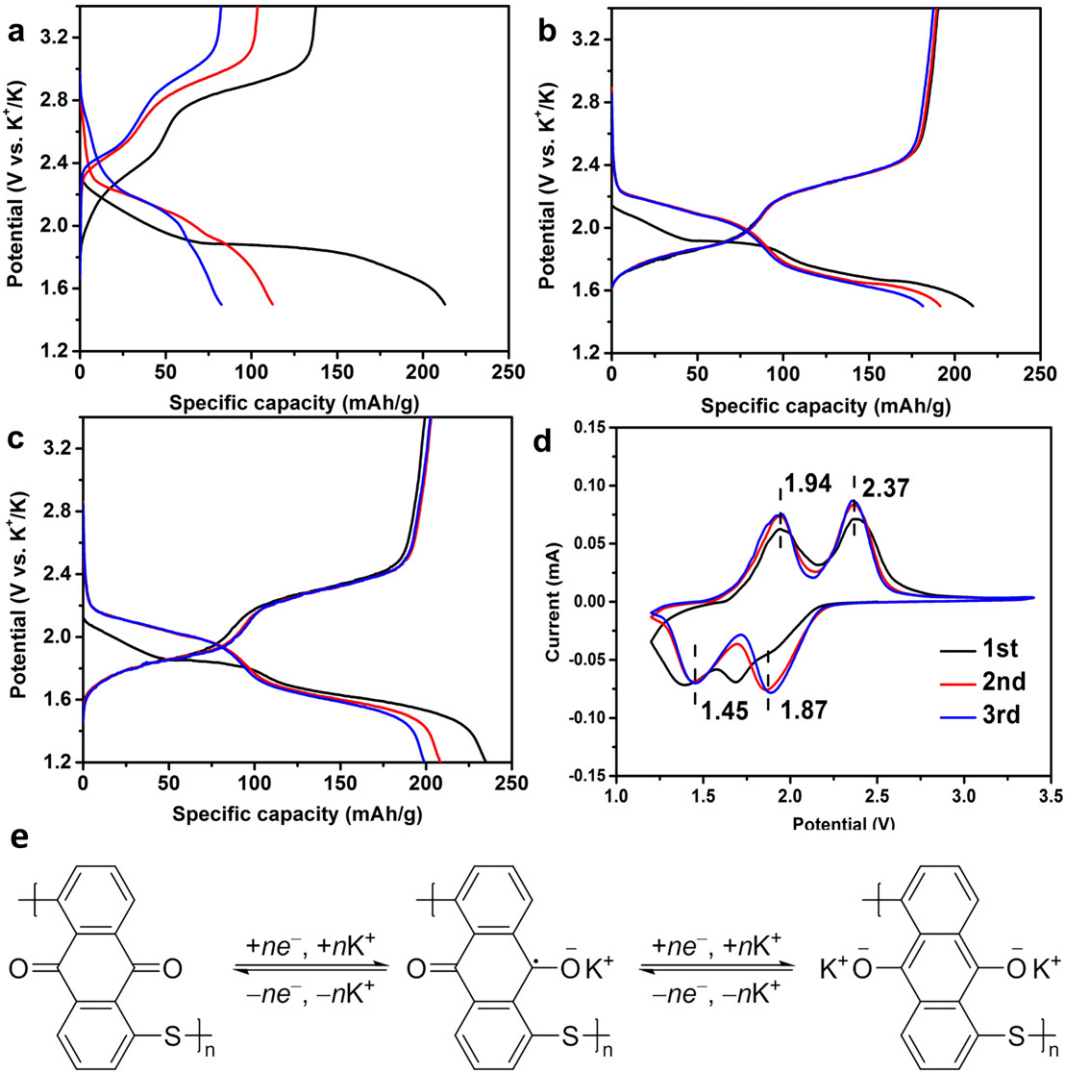

Fig. 2. (a) Charge/discharge profiles of PAQS/K cells in KPF_6/EC + DMC for the initial three cycles between 1.5 and 3.4 V at a current density of 20 mA/g, (b) Charge/discharge profiles of PAQS/K cells in KTFSI/DOL + DME for the initial three cycles between 1.5 and 3.4 V at a current density of 20 mA/g, (c) Charge/discharge profiles of PAQS/K cells in KTFSI/DOL + DME for the initial three cycles between 1.2 and 3.4 V at a current density of 20 mA/g, (d) CV curves of PAQS in KTFSI/DOL + DME for the initial three cycles between 1.2 and 3.4 V at a scan rate of 0.1 mV/s, (e) A possible redox mechanism of potassium storage in PAQS.

overlap well, where the peaks locate at the same positions: 2.37 and 1.94 V vs. K^+/K. The CV results further confirm the K^+ storage mechanism in PAQS, which corresponds to two K^+ ions inserted in two sequential steps. PAQS/Na cells also show two pairs of redox peaks, while the PAQS/Li cells present only one pair of broad redox peaks [18,19]. Therefore, the K^+ storage mechanism in PAQS is similar to that of Na, but not Li. This behavior trend is vastly different from the graphite/alkali metal cells, where graphite/Li and graphite/K show

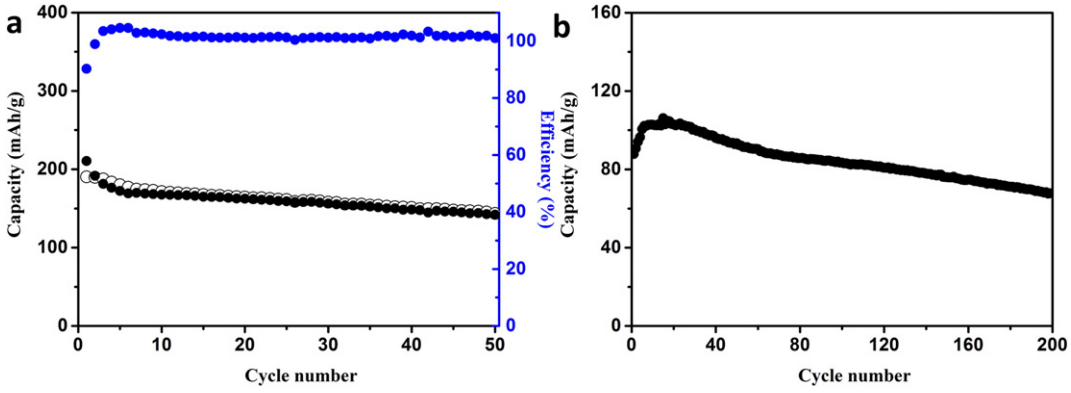

Fig. 3. (a) Cycling performance of PAQS/K cells between 1.5 and 3.4 V vs. K^+/K at a current density of 20 mA/g; (b) cycling performance of PAQS/K cells between 1.2 and 3.4 V K^+/K at a current density of 200 mA/g.

similar storage mechanisms, while Na can be barely inserted into graphite (the reversible capacity is only ~35 mAh/g) [5,21,22].

The cycling performance of PAQS/K cells in KTFSI/DOL + DME electrolyte was investigated, as shown in Fig. 3. As displayed in Fig. 3a, the PAQS electrode delivers a high reversible capacity of 190 mAh/g between 1.5 and 3.4 V vs. K^+/K at a current density of 20 mA/g, 84% of its theoretical capacity (for two K-ion insertion/extraction). It also shows a good cycling performance, with capacity retention of 75% after 50 cycles, which is better than that of the organic molecular solid —PTCDA [14]. Furthermore, the cell exhibits high coulombic efficiency, which is close to 100% after initial cycles. The cycling performance at a high current density (200 mA/g) between 1.5 and 3.4 V vs. K^+/K was also investigated. As shown in Fig. 3b, the cycling performance is relatively stable but the capacity is low, which might be due to its big particle size (see the inset of Fig. 1c). The reversible capacity is 88 mAh/g in the first cycle, then increases to 106 mAh/g and finally decreased to 68 mAh/g after 200 cycles. The mild capacity fading may be attributed to the partial dissolution of PAQS in the electrolyte, where we notice that the separator became dark yellow after 50 cycles.

4. Conclusion

In summary, PAQS was investigated as a KIB cathode material for the first time, which shows a high reversible capacity of 200 mAh/g in the KTFSI/DOL + DME electrolyte. The corresponding two slopes indicate two K-ion insertion/extraction into and from the PAQS electrode, which is similar with the mechanism of Na^+ insertion into PAQS. The PAQS/K cells show high initial coulombic efficiency (as high as 90%) and moderate cycling performance. With encouraging performance, PAQS represents a promising candidate cathode material for KIBs. Further studies will focus on improving the cycling stability and rate performance.

Acknowledgements

X. J. are thankful for the financial supports from National Science Foundation Award No. CBET-1551693. Y. Y. acknowledges financial support from the Office of Naval Research (No. N00014-13-1-0543) and National Science Foundation (CMMI-1400261).

References

[1] S.W. Kim, D.H. Seo, X. Ma, G. Ceder, K. Kang, Electrode materials for rechargeable sodium-ion batteries: potential alternatives to current lithium-ion batteries, Adv. Energy Mater. 2 (2012) 710–721.
[2] H. Pan, Y.-S. Hu, L. Chen, Room-temperature stationary sodium-ion batteries for large-scale electric energy storage, Energy Environ. Sci. 6 (2013) 2338–2360.
[3] N. Yabuuchi, K. Kubota, M. Dahbi, S. Komaba, Research development on sodium-ion batteries, Chem. Rev. 114 (2014) 11636–11682.
[4] A. Eftekhari, Potassium secondary cell based on Prussian blue cathode, J. Power Sources 126 (2004) 221–228.
[5] Z. Jian, W. Luo, X. Ji, Carbon electrodes for K-ion batteries, J. Am. Chem. Soc. 137 (2015) 11566–11569.
[6] X. Ren, Y. Wu, A low-overpotential potassium–oxygen battery based on potassium superoxide, J. Am. Chem. Soc. 135 (2013) 2923–2926.
[7] Q. Zhao, Y. Hu, K. Zhang, J. Chen, Potassium–sulfur batteries: a new member of room-temperature rechargeable metal–sulfur batteries, Inorg. Chem. 53 (2014) 9000–9005.
[8] C.D. Wessells, R.A. Huggins, Y. Cui, Copper hexacyanoferrate battery electrodes with long cycle life and high power, Nat. Commun. 2 (2011) 550.
[9] C.D. Wessells, S.V. Peddada, R.A. Huggins, Y. Cui, Nickel hexacyanoferrate nanoparticle electrodes for aqueous sodium and potassium ion batteries, Nano Lett. 11 (2011) 5421–5425.
[10] Y. Liu, F. Fan, J. Wang, Y. Liu, H. Chen, K.L. Jungjohann, Y. Xu, Y. Zhu, D. Bigio, T. Zhu, C. Wang, In situ transmission electron microscopy study of electrochemical sodiation and potassiation of carbon nanofibers, Nano Lett. 14 (2014) 3445–3452.
[11] S. Komaba, T. Hasegawa, M. Dahbi, K. Kubota, Potassium intercalation into graphite to realize high-voltage/high-power potassium-ion batteries and potassium-ion capacitors, Electrochem. Commun. 60 (2015) 172–175.
[12] W. Luo, J. Wan, B. Ozdemir, W. Bao, Y. Chen, J. Dai, H. Lin, Y. Xu, F. Gu, V. Barone, L. Hu, Potassium ion batteries with graphitic materials, Nano Lett. 15 (2015) 7671–7677.
[13] Y. Chen, W. Luo, M. Carter, L. Zhou, J. Dai, K. Fu, S. Lacey, T. Li, J. Wan, X. Han, Organic electrode for non-aqueous potassium-ion batteries, Nano Energy 18 (2015) 205–211.
[14] Z. Xing, Z. Jian, W. Luo, Y. Qi, C. Bommier, E.S. Chong, Z. Li, L. Hu, X. Ji, A perylene anhydride crystal as a reversible electrode for K-ion batteries, Energy Storage Materials 2 (2016) 63–68.
[15] J. Wu, X. Rui, G. Long, W. Chen, Q. Yan, Q. Zhang, Pushing up lithium storage through nanostructured polyazaacene analogues as anode, Angew. Chem. Int. Ed. 54 (2015) 7354–7358.
[16] P.-Y. Gu, J. Zhang, G. Long, Z. Wang, Q. Zhang, Solution-processable thiadiazoloquinoxaline-based donor-acceptor small molecules for thin-film transistors, J. Mater. Chem. C 4 (2016) 3809–3814.
[17] J. Wu, X. Rui, C. Wang, W.B. Pei, R. Lau, Q. Yan, Q. Zhang, Nanostructured conjugated ladder polymers for stable and fast lithium storage anodes with high-capacity, Adv. Energy Mater. 5 (2015) 1402189–1402194.
[18] Z. Song, H. Zhan, Y. Zhou, Anthraquinone based polymer as high performance cathode material for rechargeable lithium batteries, Chem. Commun 448-450 (2009).
[19] W. Deng, X. Liang, X. Wu, J. Qian, Y. Cao, X. Ai, J. Feng, H. Yang, A Low cost, all-organic Na-ion battery based on polymeric cathode and anode, Scientific Reports, 3, 2013.
[20] J. Bitenc, K. Pirnat, T. Bančič, M. Gaberšček, B. Genorio, A. Randon-Vitanova, R. Dominko, Anthraquinone-based polymer as cathode in rechargeable magnesium batteries, ChemSusChem 8 (2015) 4128–4132.
[21] T. Ohzuku, Y. Iwakoshi, K. Sawai, Formation of lithium-graphite intercalation compounds in nonaqueous electrolytes and their application as a negative electrode for a lithium ion (shuttlecock) cell, J. Electrochem. Soc. 140 (1993) 2490–2498.
[22] R. Asher, S. Wilson, Lamellar compound of sodium with graphite, Nature, 181, 1958.